

This is an Open Access document downloaded from ORCA, Cardiff University's institutional repository:<https://orca.cardiff.ac.uk/id/eprint/84434/>

This is the author's version of a work that was submitted to / accepted for publication.

Citation for final published version:

Shao, Longyi, Hou, Cong, Geng, Chunmei, Liu, Junxia, Hu, Ying, Wang, Jing, Jones, Tim, Zhao, Chengmei and Berube, Kelly 2016. The oxidative potential of PM10 from coal, briquettes and wood charcoal burnt in an experimental domestic stove. *Atmospheric Environment* 127, pp. 372-381.
10.1016/j.atmosenv.2015.12.007

Publishers page: <http://dx.doi.org/10.1016/j.atmosenv.2015.12.007>

Please note:

Changes made as a result of publishing processes such as copy-editing, formatting and page numbers may not be reflected in this version. For the definitive version of this publication, please refer to the published source. You are advised to consult the publisher's version if you wish to cite this paper.

This version is being made available in accordance with publisher policies. See <http://orca.cf.ac.uk/policies.html> for usage policies. Copyright and moral rights for publications made available in ORCA are retained by the copyright holders.



The oxidative potential of PM₁₀ from coal, briquettes and wood charcoal burnt in an experimental domestic stove

Longyi Shao ^{1*}, Cong Hou ¹, Chunmei Geng ², Junxia Liu ³, Ying Hu¹, Jing Wang ², Tim Jones ⁴, Chengmei Zhao¹, Kelly Bérubé ⁵

1. State Key Laboratory of Coal Resources and Safe Mining, School of Geosciences and Survey Engineering, China University of Mining and Technology (Beijing), Beijing 100083, China;

2. Chinese Research Academy of Environmental Sciences, Beijing 100012, China;

3. China Association of Resource Comprehensive Utilization, Beijing 100082, China.

4. School of Earth and Ocean Sciences, Cardiff University, Park Place, Cardiff, UK

5. School of Biosciences, Cardiff University, Museum Avenue, Cardiff, UK

** Email: ShaoL@cumtb.edu.cn*

Highlights:

1. Burning raw powdered coal emits more PM than burning honeycomb briquette.
2. The PM₁₀ emitted by burning honeycomb briquettes had a higher oxidative potential.
3. The water-soluble heavy metals in PM₁₀ were associated with high oxidative potential.
4. Burning raw powdered coal had a higher health risk than burning honeycomb briquette.

Abstract: Coal contains many potentially harmful trace elements. Coal combustion in unvented stoves, which is common in most parts of rural China, can release harmful emissions into the air that when inhaled cause health issues. However, few studies have dealt specifically with the toxicological mechanisms of the particulate matter (PM) released by coal and other solid fuel combustion. In this paper, PM₁₀ particles that were generated during laboratory stove combustion of raw powdered coal, clay-mixed honeycomb briquettes, and wood charcoal were analysed for morphology, trace element compositions, and toxicity as represented by oxidative DNA damage. The analyses included Field Emission Scanning Electron Microscopy (FESEM),

Inductively Coupled Plasma Mass Spectrometry (ICP-MS) and Plasmid Scission Assay (PSA). Gravimetric analysis indicated that the equivalent mass concentration of PM₁₀ emitted by burning raw powdered coal was higher than that derived by burning honeycomb coal. FESEM observation revealed that the coal burning-derived PM₁₀ particles were mainly soot aggregates. The PSA results showed that the PM₁₀ emitted by burning honeycomb briquettes had a higher oxidative capacity than that from burning raw powdered coal and wood charcoal. It is also demonstrated that the oxidative capacity of the whole particle suspensions were similar to those of the water soluble fractions; indicating that the DNA damage induced by coal burning-derived PM₁₀ were mainly a result of the water-soluble fraction. An ICP-MS analysis revealed that the amount of total analysed water-soluble elements in the PM₁₀ emitted by burning honeycomb briquettes was higher than that in PM produced by burning raw powdered coal, and both were higher than PM from burning wood charcoal. The total analysed water-soluble elements in these coal burning-derived PM₁₀ samples had a significantly positive correlation with the level of DNA damage; indicating that the oxidative capacity of the coal burning-derived PM₁₀ was mainly sourced from the water soluble elements. The water-soluble As, Cd, Ge, Mn, Ni, Pb, Sb, Se, Tl, and Zn showed the highest correlation with the oxidative potential, implying that these elements in their water soluble states were the primary responsible factor for the plasmid DNA damage. The exposure risk was further assessed using the particle mass concentrations multiplied by the percent of DNA damage under the dose of 500 µg ml⁻¹. The results revealed that the exposure risk of burning raw powdered coal was much higher than that of burning honeycomb coal.

Key words: plasmid scission assay; inductively coupled plasma mass spectrometry (ICP-MS); coal burning-derived PM₁₀; oxidative potential; water-soluble elements; exposure risk

1. Introduction

Emissions from coal combustion represent an important source of gaseous and particulate pollutants in the atmosphere, and these pollutants can have a significant impact on atmospheric chemistry, climate change, and human health (Dockery et al., 1993; Levine et al., 1995; Samet

et al., 2000; Andreae and Merlet, 2001; Kan et al., 2007, 2012; Jones et al., 2009). Epidemiological investigations have demonstrated the association between exposure to particulate matter (PM) and an increased incidence of mortality and morbidity from lung cancer and cardiovascular diseases (Crabbe, et al., 2012; Xu et al., 2003; Hoek et al., 2013; Kheirbek, et al., 2013; Shao et al., 2013). Recently, a literature review by Pui et al. (2013) demonstrated that the components in PM_{2.5} from coal combustion and from vehicle emissions are the dominant contributors to regional haze in China; they also demonstrated that short-term exposure to PM_{2.5} is strongly associated with an increased risk of morbidity and mortality from cardiovascular and respiratory diseases in China. Smoky coal used domestically indoors in China is a known human carcinogen, and outdoor air containing coal-burning emissions is also considered as a potential human lung carcinogen, (Loomis et al., 2013).

China is the largest coal producer and consumer in the world. In 2013, China produced 3.7 billion tons of coal and consumed approximately 3.61 billion tons of coal (China Statistical Yearbook, 2013), which was equal to approximately 68% of the primary energy consumed in China. Residential coal stoves are commonly used for cooking and heating, especially in the winter. Approximately 25% of the coal production in China is high-sulphur coal, with a sulphur content exceeding 2%, and the burning of these high-sulphur coals releases SO₂, together with NO₂ and PM₁₀ into the atmosphere, resulting in atmospheric pollution (Luo, 2008; Chen et al., 2009). Furthermore, coal contains many potentially harmful trace elements that may be minimal on average, but can be enriched as a result of special geologic conditions (Bogdanovic et al., 1995; Xu et al., 2003; Dai et al., 2003; Shao et al., 2003; Tang et al., 2004; Ren et al., 2006; Li et al., 2006). During the combustion, processing, and utilization of coal, these trace elements can be released into the air, causing harm to the environment and human health (Neas, 2000). Although we know that coal combustion can release harmful substances into the air, the toxicological mechanisms of the inhaled PM released by coal-combustion is still not clear. Although toxic metals are found to be associated with some types of coals (Tang et al., 2004; Ren et al., 2006), it is still unclear which elements emitted during coal combustion are of most concern in terms of their toxicity.

A number of studies have shown that atmospheric PM₁₀, in which coal-burning particles

dominate, is implicated in increased morbidity and mortality and can cause asthma, respiratory disease, and respiratory inflammation; it can even involve the cardiovascular system, nervous system, immune system and may eventually cause cancer (Zhang et al., 2003; Ostro et al. 2006; Lin et al. 2007; Loomis et al., 2013). Although the biological mechanisms underlying the induction of lung cancer by PM₁₀ have been examined extensively (Straif et al., 2006; Benbrahim-Tallaa et al., 2012; Loomis et al., 2013), the role played in these adverse health effects by coal burning-derived PM₁₀ remain unclear. A widely accepted hypothesis is that oxidative damage originates from the bioreactive surface of airborne particles (Donaldson et al., 1996; Li et al., 1997; Shao et al., 2007); the bioavailable transition metals on the surface of airborne particles could activate oxidants that could damage DNA (Costa et al., 1997; Greenwell et al., 2003; DiStefano et al., 2009; Sánchez-Pérez et al., 2009; Vidrio et al., 2009; Zhong et al., 2010). Many other studies have also shown that soluble metal components produce Reactive Oxygen Species (ROS), which can induce oxidative stress and inflammation in the lungs and respiratory tract (See et al., 2007; Distefano et al., 2009; Vidrio et al., 2009; Zhong et al., 2010). The USA Environmental Protection Agency (USEPA) defines Zn and Pb as toxic elements, and Zn is regarded as a bioreactive element (Adamson et al., 2000). Other studies have also indicated that Zn is likely to be a major element responsible for particle-induced plasmid DNA damage (Greenwell et al., 2003; Shao et al., 2006, 2007; Lu et al., 2006). Lan and co-workers (2004) demonstrated oxidative damage-related genes (e.g. *AKR1C3* and *OGG1*) modulated risks for lung cancer due to exposure to PAH-rich coal combustion emissions. Their human molecular epidemiology study took place in Xuan Wei County, China, which had the highest lung cancer rates in China. It was demonstrated that PAHs were activated to genotoxic intermediates to produce PAH metabolites that form DNA adducts or reactive oxygen species (ROS) leading to oxidative DNA damage, such as 8-hydroxy-2'-deoxyguanosine (8-oxo-dG).

Currently, many methods are employed in the toxicological study of atmospheric particles; such as irrigation, the Ames test method, micronucleus experiments, chromosome aberration tests, and the comet assay. However, most of these are only qualitative techniques. In recent years, a plasmid DNA scission assay has been developed to study the toxicity of atmospheric

particulates (Li et al., 1997; Whittaker, 2003; Shao et al., 2007; Chuang et al., 2011, 2013); it is a simple, rapid, high-sensitivity technique to detect DNA damage and allows for the toxicity of particles to be quantified. This method has been proved to be effective in characterizing the oxidative capacity of coal burning-derived particles (Wang et al., 2014). Inductively Coupled Plasma Mass Spectrometry (ICP-MS) can be used to measure the levels of the water-soluble trace elements responsible for the particle-induced DNA damages (Shao et al., 2006).

This paper evaluates the oxidative damage to plasmid DNA by PM₁₀ generated by laboratory-stove combustion of different types of Chinese coal. The water-soluble trace elements of PM₁₀ were examined using ICP-MS. The aim of this paper was to assess the toxicity of coal burning-derived PM₁₀ and the relationship between the particle-induced oxidative potential and the metal compositions of these coal burning-derived PM₁₀.

2. Sampling and experiments

2.1 Combustion system and sample collection

The coals that were used in these experiments were collected from a number of coal mining areas, including Zhijin in Guizhou Province (ZJ), Datong in Shanxi Province (DT), Dongsheng in the Inner Mongolia Autonomous Region (DS), Yinchuan in the Ningxia Hui Autonomous Region (YC), and Jingxi (western Beijing mountain) in Beijing (JX). Raw, loose, powdered coals were prepared from ZJ, DT, DS, YC, and JX, and the clay-mixed honeycomb briquettes were prepared from ZJ and DT by a combination of 80% raw powdered coals and 20% clay. Wood charcoal was used as a comparison in the experiments. Information about the proximate and ultimate analyses of raw powdered coals used in this study is given in Table 1.

We used a laboratory-made combustion system to conduct the burning experiments, which were carried out at the Laboratory of the Chinese Research Academy of Environmental Sciences (Geng et al., 2012). The system was composed of a combustion stove with smoke dilution tunnels and smoke chambers. The coal-stove, which is used widely for domestic cooking and heating in China, was purchased from the grocery market. It has a metallic outer cover and thermal-insulated ceramic liner. The cylindrical inner volume is 0.01 m³. The dilution tunnel consisted of two main parts made of stainless steel, including an orthogonal

pipe and a cylindrical tunnel, and an attached suction fan. The orthogonal pipe with a length of 1 m and a radius of 20 cm was connected to the stove for flue gas introduction and first-step dilution with filtered air. At the end of the orthogonal pipe, a horizontal cylindrical tunnel with a length of 4 m and a radius of 40 cm was connected for second-step dilution. At the end of the tunnel, there were several outlets for suction fans and sampling. The flow rate of the suction fan was controlled by a Venturic tube and was fixed at 5800 L/min. The residence time of flue gas in the dilution tunnel was 5.5 second. After second-step dilution, the temperature of diluted flue gas decreased to 30°C. The smoke chamber connected to the horizontal cylindrical tunnel was used for real-time measurement of gaseous and particulate pollutant during the combustion experiments. Our PM₁₀ sampler was connected to this smoke chamber. During the experiments, the flow rate of the diluted flue gas into smoke chamber was fixed at 100 L/min.

Coal samples were ignited in the stove using pre-weighed wood charcoal (0.5 kg). To minimise the influence of charcoal burning emissions, the coal samples (1.0 kg for each experiment) were put into the stove until smoking from charcoal combustion stopped. Sampling started when the raw coal samples were put into the stove and ended when the combustion was complete, and the whole process lasted for approximately one hour. The schematic diagram showing this combustion system is shown in Figure 1.

A medium-volume particle sampler (Dickel-80, Beijing Geological Instrument Dickel Cooperation limited, China) and a MinivolTM particle sampler (Air Metric, U.S.A), which were connected to the dynamic smoke chamber, were used to collect the particulate matter. Particles with an aerodynamic diameter of 10 µm or less were collected. Quartz fibre filters (diameter 90 mm) were used in the Dickel-80 sampler (flow rate 78 L/min), and were used for the plasmid scission assay and ICP-MS experiments. Polycarbonate filters (diameter 47 mm) were used in the Minivol sampler (the flow rate was 5 L/min), and were used for the Field Emission Scanning Electron Microscopy (FESEM).

2.2 FESEM analysis

A Field Emission Scanning Electron Microscope (FESEM) (JSM-6700F) was used to investigate the morphology of the particles. Approximately one eighth of each polycarbonate

filter was cut and then mounted onto a copper washer using epoxy resin. The specimen was gold-coated to a thickness of 20 nm. Secondary electron images were obtained to analyse the morphology of the burning-derived PM₁₀ particles.

2.3 Plasmid Scission Assay

The plasmid scission assay is an *in-vitro* method for assessing and comparing the oxidative potential of inhalable particles (Greenwell et al., 2003; Reche et al., 2012; Xiao et al., 2013; Chuang et al., 2013; Sun et al., 2014). The assay is based on the principle that any free radicals associated with particle surfaces can damage the supercoiled DNA by “nicking” the strands. This damage initially causes the DNA to unwind from being supercoiled into a relaxed coil. Further damage results in linearization followed by complete fragmentation. This change in structure alters the electrophoretic mobility of the DNA, thereby allowing for separation and quantification on an agarose gel.

A detailed experimental procedure has been described in Merolla and Richards (2005), Shao *et al.* (2006), Reche *et al.* (2012) and Chuang et al. (2013). The PM₁₀ samples, together with a procedural blank filter, were incubated in HPLC-grade water. The incubations were gently agitated in a vortex mixer (Scientific Industries, Vortex Genie 2) for 20 h at room temperature to ensure the maximum mixing of the PM₁₀ sample in water and to avoid sedimentation. At this stage after incubation each sample was separated into two parts; one part was taken to directly represent the intact whole-particle suspension, and another part was used to prepare the water-soluble fraction. The water-soluble fraction of PM₁₀ sample was obtained by spinning the intact whole-particle suspension in a centrifuge (D37520, Germany) at 13000r/min for 80 minutes. At the end of this centrifuging, the supernatant was collected using a pipette; this supernatant represented the soluble fraction of the PM₁₀ samples. The plasmid scission assay was used for both the intact whole-particle suspension and the centrifuged water-soluble fraction of the PM₁₀ sample. Each of them was sequentially diluted into five particle dosages; 25, 50, 100, 300, and 500 µg ml⁻¹ respectively. All of the dose-scaled incubations were calibrated into a final volume of 20 µl, each containing 200 ng of φX174-RF DNA (Promega Corporation, USA). The prepared dose-scaled incubations were gently agitated in a vortex mixer for another 6 h to ensure the maximum mixing of the PM₁₀ sample with DNA. At this

stage, bromophenol blue dye (3.5 μ l) was added to each dose-scaled sample before injecting the sample into the gel which is composed of 0.6% agarose and 0.25% ethidium bromide. Then the gel carrying the injected samples was placed in a 30 V electrophoretic voltage for 16 h at room temperature in a 1% tris-borate-EDTA (TBE) buffer. The electrophoresis gels were photographed and a densitometric analysis was performed using the Genetools program (TRANSILLUMINATOR 2020D). A semi-quantitative protocol was established that measured the relative proportion of damaged DNA (relaxed and linearized) in each lane of the gel, and was expressed as a percentage of the total DNA in each lane. Two replicates of each lane were quantified in this way, and the means were recorded for each particle dosages. Subtracting the damage caused by the negative control (HPLC-grade water), the DNA damage that was induced by the airborne particles at different dosages was calculated.

To guarantee the accuracy of the experiment result, we analysed one procedural blank quartz fibre filter. The oxidative damage to plasmid DNA induced by the blank quartz fibre filter was below 10%, so it was considered that the quartz filter does not have a significant influence on the experimental results. In addition, the water-soluble fraction obtained after centrifuging will have had any broken quartz filter shards removed, thus avoiding any extra oxidative damage.

2.4 ICP-MS analysis

This study used a high-resolution Inductively Coupled Plasma Mass Spectrometer (model number: ELEMENT; Manufacturer: Finnigan-MAT company) for the analysis of trace elements from coal burning-derived PM₁₀ with a detection limit of 1ppt~1ppb (10^{-12} ~ 10^{-9}). The experiments were carried out at a laboratory in the Beijing Research Institute of Uranium Geology. The procedure used was based on Shao et al. (2013). Water-soluble trace elements were obtained by directly analysing the water-soluble fractions of the PM₁₀ samples that were previously processed by centrifugation before the plasmid scission assay. The results were reported as a concentration of the element in its soluble form in the intact PM₁₀ sample, which were expressed in ppm by weight.

3 Results

3.1 Mass concentration and particle morphology of the coal burning-derived PM₁₀

In order to investigate the relative amounts of PM₁₀ emitted by burning different fuels, the equivalent (equal amount of fuel, equal time of combustion, and equal combustion conditions) mass concentration of the coal burning-derived PM₁₀ were estimated by combining the sampling air volume and the loaded PM₁₀ mass in filters. The equivalent mass concentration can be calculated by following formula:

$$MC(\mu\text{g} / \text{m}^3) = \frac{M_2 - M_1}{V}$$

In this formula, MC represented equivalent mass concentration of the coal burning-derived PM₁₀ (μg/m³), M₁ represented the mass of the quartz fibre filters before sampling (μg), M₂ represented the mass of the quartz fibre filters loaded with particles after sampling (μg), V represented the sampling volume (m³), which was the value of sampling time multiplied by the flow rate of the sampler.

Table 2 showed the mass concentrations of the PM₁₀ emitted by burning different coals. The mass concentration of the coal burning-derived PM₁₀ varied greatly, ranging from 689 μg/m³ for the DT honeycomb briquette to 10694 μg/m³ for the DS raw powdered coal. The mass concentrations of the PM₁₀ emitted by burning honeycomb briquette were from 689 μg/m³ to 1282 μg/m³, and averaged 986 μg/m³. The mass concentrations of the PM₁₀ emitted by raw powdered coal were from 1436 μg/m³ to 10694 μg/m³, and averaged 5251 μg/m³. This result demonstrated that the mass concentration of PM₁₀ emitted by burning raw powdered coal was higher than that by burning honeycomb briquette.

FESEM observation revealed that the morphology types of coal burning-derived particles were almost all soot aggregates, which consisted of many carbon spheres. Figure 2 demonstrates that the number density per unit area in the images of the PM₁₀ emitted by burning honeycomb briquette was relatively small, while number density per unit area in the images of the PM₁₀ emitted by burning raw powdered coal was much denser. This reconfirmed that burning raw powdered coal would generate more particles than burning honeycomb briquettes.

3.2 Oxidative potential of PM₁₀ generated from burning different types of coal

The oxidative potential of the PM₁₀ generated by burning honeycomb briquettes, the raw powdered coals, and the wood charcoal were examined with a plasmid scission assay. A total of 8 types of PM₁₀ samples were used in this study and represented emissions from burning raw powdered coals from ZJ, DT, DS, YC, and JX, the clay-mixed honeycomb briquettes from ZJ and DT, and wood charcoal. The gel images and histograms shown in Figure 3 and Table 3 provide a quantitative analysis of the oxidative DNA damage induced by a whole-particle suspension and a water-soluble fraction in five particle doses (25, 50, 100, 300, 500 µg ml⁻¹). It can be seen that with increasing doses, the particle-induced DNA damage for all of the coal burning-derived PM₁₀ types showed a general increasing trend. A positive dose-response relationship exists between the amounts of DNA damages and the sample doses, which implies that higher mass concentrations of PM in the ambient air could cause a higher oxidative potential, and thus a higher toxicity per cubic metre of air.

The amount of damage to the plasmid DNA that was induced by coal burning-derived PM₁₀ varied from 5% to 55%. Table 3 and Figure 3 also demonstrated that, under the same dose (Table 3), the oxidative potential of both the whole-particle suspension and the water-soluble fraction of the PM₁₀ followed a clear pattern. High from the ZJ and DT honeycomb briquettes emissions, moderately high from the YC and ZJ powdered coals emissions, and relatively low from the DT, DS, and JX powdered coals and wood charcoal emissions.

It was found that the oxidative potential of the PM₁₀ generated from burning honeycomb briquettes was significantly higher than that generated by burning the corresponding raw powdered coals. At a particle dose of 500 µg ml⁻¹, the PM₁₀ generated from burning ZJ and DT honeycomb briquettes induced DNA damage of 55% and 46% by their whole-particle suspension respectively, which was higher than the damage percentages of 34% and 19% from their corresponding raw powdered coals.

Furthermore, the differences between the amount of DNA damage induced by the whole-particle suspension and the corresponding water-soluble fraction of the PM₁₀ samples at all dose levels were relatively small. Figure 4 shows a comparison between the amount of DNA

damage resulting from the whole-particle suspension and from the soluble fraction of the coal burning-derived PM₁₀ at a dose of 500 µg ml⁻¹; it is clear that the differences between the amount of DNA damage induced by the whole-particle suspension and by the corresponding water-soluble fraction of these PM₁₀ were mostly insignificant, ranging from 4% to 30%, but mostly less than 20%. The amount of damage induced by the soluble fraction can contribute more than 70% to the amount of damage induced by the whole-particle suspension. This result indicates that the oxidative potential of the PM₁₀ generated by coal burning-derived is mainly sourced from their water-soluble components.

3.3 Trace elements in the PM₁₀ emitted by burning different coals

An ICP-MS was used to detect the concentration of elements in the coal burning-derived PM₁₀. The elements analysed included As, Cd, Co, Cr, Cs, Cu, Ge, Mo, Mn, Ni, Pb, Sb, Se, Sr, Ti, Tl, V, and Zn. The concentrations of these elements in their water-soluble fractions were analysed and the results were reported in weight ppm of each element in its soluble state in the original intact PM₁₀ samples (Table 4).

For the total analysed water-soluble elements, the PM₁₀ emitted by burning the ZJ honeycomb briquette had the highest level (21480.63 ppm), followed by those emitted by burning the DT honeycomb briquette (5658.73 ppm). For coal samples the values were YC powdered coal (3960.71 ppm), the ZJ powdered coal (3196.05 ppm), the DT powdered coal (219.28 ppm), the DS powdered coal (212.65 ppm), the JX powdered coal (201.52 ppm), and the wood charcoal (140.11 ppm) in descending order. It is clear that the PM₁₀ particles emitted by burning honeycomb briquettes produced a higher content of total analysed water-soluble trace elements than those emitted by burning raw powdered coals, with the lowest values being the PM₁₀ emitted by burning wood charcoal.

Table 4 also showed that the PM₁₀ emitted by burning honeycomb briquettes was enriched with water-soluble elements such as As, Cd, Cu, Ge, Mn, Ni, Pb, Se, Sb, Ti, Tl, V, and Zn. All of these elements were present at concentrations greater than 10 ppm, and the water-soluble As, Ge, Pb, Tl, and Zn were present at levels greater than 100 ppm. For the raw powdered coals, the coal burning-derived PM₁₀ was enriched with water-soluble As, Cu, Ni, Pb, Ti, and Zn; these individual elements reached levels that were greater than 10 ppm.

4 Discussion

4.1 Relationship between the oxidative potential and the content of water-soluble trace elements

To examine the most probable source of the oxidative potential of the coal burning PM₁₀, the amounts of DNA damage were correlated with corresponding concentrations of the water-soluble elements in the intact PM₁₀ samples. As the DNA damage values from all particle doses showed the same trend, we only choose one dose level (500 µg ml⁻¹) for the correlation analysis. The Pearson correlation coefficients are provided in Table 5, with a sample number n=8 and a threshold correlation coefficient of 0.71 at 95% confidence level.

The particle-induced oxidative potential displayed a significant positive correlation with the total analysed water-soluble metal concentrations with a Pearson correlation coefficient of 0.87, implying that the oxidative potential of coal burning-derived PM₁₀s was derived mainly from its water-soluble elements. This finding was also supported by the fact that the whole-particle suspension of these coal burning-derived PM₁₀ induced similar amounts of DNA damages relative to their corresponding water-soluble fractions.

The correlation coefficients between the particle-induced oxidative potentials from a dosage of 500 µg ml⁻¹ and the concentrations of individual water-soluble heavy metals in PM (Table 5) can be used to determine which individual elements were most responsible for the particle-induced oxidative potential of these coal burning-derived PM₁₀. The water-soluble As, Cd, Ge, Mn, Ni, Pb, Sb, Se, Tl, and Zn exhibited relatively significant positive correlations with the oxidative potential (correlation coefficients higher than 0.71), indicating that these elements in their water-soluble states were likely responsible for the plasmid DNA damage. Similar conclusions have been reached by other reports for PM₁₀ from Beijing (Shao et al., 2006, Sun et al., 2014) and in the UK (Moreno et al., 2004; Merolla and Richards, 2005; Reche et al., 2012).

Some previous studies (Querol et al., 2006; Liu et al., 2010) have shown that heavy metal pollutants, such as Cr, Zn, Pb, and Mn, can be produced from combustion-related industry. Tang and Huang (2004) and Ren et al.(2006) found that high levels of As, Se, Zn and Pb might

be sourced from the combustion of different types of coal, and all of these elements are considered to be potentially harmful to human health. The results of this study demonstrated the occurrence of Cr and Zn, and to a lesser extent Pb and Mn in coal burning-derived PM₁₀; although this does depend on the geochemistry of the original coal.

4.2 Possible causes of the variation in the oxidative potential of coal burning-derived PM₁₀.

The PM₁₀ emitted by burning honeycomb briquettes had a higher content of total analysed water-soluble trace elements and a higher oxidative potential than those emitted by burning raw powdered coals. This can be attributed to the clay mixed into the briquettes, which would enrich the inorganic elements in the PM₁₀, effectively being released as fly ash.

For the intact powdered coals, the variations in the oxidative potential could be explained by the raw coal quality; especially in terms of the difference in the sulphur and ash content. The higher percentages of total water-soluble trace elements and the higher oxidative potential of the PM₁₀ emitted by burning ZJ powdered coal can be attributed to the higher sulphur content of the raw ZJ coal (Table 1). The sulphur-rich coals of the Late Permian age from the Zhijin coal mining area of southwestern China normally contain higher levels of pyritic sulphur that tends to be associated with some toxic heavy metals (Ren et al., 2006). Therefore, the PM₁₀ emitted by burning high-sulphur coal would have higher percentages of trace elements and a higher oxidative potential.

The PM₁₀ that was emitted by burning YC powdered coal also had higher percentages of total water-soluble trace elements and a higher oxidative potential. This could have been because the YC powdered coal had a higher ash content (Table 1). The high coal ash content tends to be accompanied by higher levels of certain trace elements (Ren et al., 2006). This finding allows us to infer that the PM₁₀ emitted by burning high-ash coals can be associated with a relatively high percentage of water-soluble trace elements, thereby inducing a high oxidative potential. The JX coal had high ash content but was associated with a lower PM₁₀-induced oxidative potential. This is due to the lower sulphur content in the raw coal.

4.3 Exposure risk of the PM₁₀ emitted by burning different coal types

In order to elucidate the exposure risk to humans we devised a toxicity index to represent

the relative risk for people exposed to the ambient air with different types of coal burning-derived PM₁₀:

$$TI = MC \times P_{DNA}$$

In this formula, *TI* represents toxicity index, *MC* represents the mass concentration of the coal burning-derived PM₁₀, *P_{DNA}* represented the percentage of DNA damage at the 500 µg/ml PM₁₀ dose. Table 6 showed that the *TI* of the PM₁₀ emitted by burning YC raw powdered coal and DS raw powdered coal were much higher than that by burning other types of coals. It can also been seen that the *TI* values of the PM₁₀ emitted by burning ZJ and DT honeycomb briquettes, (70987 and 31754 respectively) were clearly lower than those by burning their corresponding raw powdered coals (96577 and 80265 respectively). This result indicated that exposure to the PM₁₀ emitted by burning raw powdered coals is associated with higher risks to human health than exposure to the PM₁₀ emitted by burning honeycomb briquettes.

5. Conclusion

1) Burning raw powdered coal emits more PM₁₀ than burning honeycomb briquette. The oxidative potential of the PM₁₀ emitted by burning honeycomb briquettes was significantly higher than that by burning raw powdered coals and wood charcoal.

2) The PM₁₀ emitted by burning honeycomb briquettes had a higher content of total water-soluble trace elements than that emitted by burning raw powdered coals and wood charcoal. The PM₁₀ particles emitted by burning honeycomb briquettes were enriched with water-soluble As, Ge, Pb, Tl, and Zn, and the PM₁₀ particles emitted by burning raw powdered coals was enriched with water-soluble As, Cu, Ni, Pb, Ti, and Zn.

3) The oxidative potential of the coal burning-derived PM₁₀ was mainly sourced from their water-soluble fractions. The water-soluble As, Cd, Ge, Mn, Ni, Pb, Sb, Se, Tl, and Zn showed the most significant correlation with the oxidative potential, implying that these elements in their water-soluble states were responsible for the particle-induced DNA damage.

4) The PM₁₀ emitted by burning coals with high levels of mixed clay, sulphur, and ash is associated with a correspondingly high percentage of water-soluble trace elements, thereby

inducing a high oxidative potential.

5) The exposure risk to humans from the PM₁₀ emitted by burning raw powdered coal was significantly higher than that from burning honeycomb briquette emissions.

Acknowledgements

This work was supported by the National Basic Research Program of China (Grant No. 2013CB228503) and the National Natural Science Foundation of China (Grant No. 41175109).

Two anonymous reviewers are thanked for their helpful comments.

References

- Adamson I Y R, Prieditis H, Hedgecock C. Vincent R. Zinc is the toxic factor in the lung response to an atmospheric particulate sample. *Toxicology and Applied Pharmacology* 2000; 166: 111–119.
- Andreae M O, Merlet P. Emission of trace gases and aerosols from biomass burning. *Global Biogeochemical Cycles* 2001; 15: 955-966.
- Benbrahim-Tallaa, L., Baan, R.A., Grosse, Y., Lauby-Secretan, B., Ghissassi, F.E., Bouvard, V., Guha, N., Loomis, D., Straif, K.. Carcinogenicity of diesel-engine and gasoline-engine exhausts and some nitroarenes. *The Lancet Oncology* 2012; 13: 663-664.
- Bogdanovic I, Fazinic S, Itkos S, et al.. Trace element characterization of coal fly ash particle. *Nuclear Instrument and Methods in Physics Research B* 1995; 99: 402-405.
- Geng, C., Wang, K., Wang, W., Chen, J., Liu, X., Liu, H.. Smog chamber study on the evolution of fume from residential coal combustion. *Journal of Environmental Sciences* 2012; 24: 169-176.
- Chen Y Q, Liu H. The analysis of toxic trace elements in coal and fly ash in the region of Beijing. *Comprehensive Utilization Of Fly Ash* 2009; 3: 20-22.
- China Statistic Department. *China Statistics Yearbook* 2013.
- Chuang H C, Jones T, Lung S C, Bérubé K A. Soot-driven reactive oxygen species formation from incense burning. *Science of Total Environment* 2011; 409: 4781-4787.
- Chuang H C, Bérubé K A, Lung S C, Bai K J, Jones T. Investigation into the oxidative potential generated by the formation of particulate matter from incense combustion. *Journal of Hazardous Materials* 2013; 244-245: 142-150.
- Costa D L, Dreher K L. Bioavailable transition metals in particulate matter mediate cardiopulmonary injury in healthy and compromised animal models. *Environmental Health Perspectives* 1997; 105: 1053–1060.
- Crabbe H. Risk of respiratory and cardiovascular hospitalization with exposure to bushfire particulates: new evidence from Darwin, Australia. *Environmental Geochemistry and Health* 2012; 34: 697-709.
- Dockery D W, Pope III A, Xu X, Spengler J D, Ware J H, Fay M E, Ferris B G, Jr., Speizer F E. An association between air-pollution and mortality in 6 United-States cities. *The New England Journal of Medicine* 1993; 329: 1753-1759.
- Dai S F, Ren D Y, Liu J R, Li S S. The occurrence and distribution of toxic trace elements in the coal of Fengfeng mine of Hebei Province. *Journal of China University of mining and technology* 2003; 32(4):

358-361.

Distefano E, Eiguren-Fernandez A, Delfino R J, Sioutas C, Froines J R, Cho A K. Determination of metal-based hydroxyl radical generating capacity of ambient and diesel exhaust particles. *Inhalation Toxicology* 2009; 21: 731-738.

Donaldson K, Beswick P H, Gilmour P S. Free radical activity associated with the surface of the particles: a unifying factor in determining biological activity. *Toxicology Letters* 1996; 88: 293-298.

Greenwell L L, Moreno T, Richard R J. Pulmonary antioxidants exert differential protective effects against urban and industrial particulate matter. *Journal of Biosciences* 2003; 28: 101-107.

Hoek G, Krishnan RM, Beelen R, Peters A, Ostro B, Brunekreef B, Kaufman J D. Long-term air pollution exposure and cardio-respiratory mortality: a review. *Environmental Health* 2013; 12: 43.

Jones T, Wlodarczyk A, Koshy L, Brown P, Shao L Y, Bérubé K. The geochemistry and bioreactivity of fly-ash from coal-burning power stations. *Biomarkers* 2009; 14(S1): 45-48.

Kan H, London S, Chen G, Zhang Y, Song G, Zhao N, Jiang L, Chen B. Differentiating the effects of fine and coarse particles on daily mortality in Shanghai, China. *Environment International* 2007; 33: 376-384.

Kan H, Chen R, Tong S. Ambient air pollution, climate change, and population health in China. *Environment International* 2012; 42: 10-19.

Kheirbek I, Wheeler K, Walters S, Kass D, Matte T. PM_{2.5} and ozone health impacts and disparities in New York City: sensitivity to spatial and temporal resolution. *Air Quality, Atmosphere and Health* 2013; 6: 473-486.

Lan Q, Mumford J L, Shen M, Demarini D M, Bonner M R, He X, Yeager M, Welch R, Chanock S, Tian L, Chapman R S, Zheng T, Keohavong P, Caporaso N, Rothman N. Oxidative damage-related genes AKR1C3 and OGG1 modulate risks for lung cancer due to exposure to PAH-rich coal combustion emissions. *Carcinogenesis* 2004; 25(11): 2177-2181.

Levine J S, Cofer W R, Cahoon D R, Winstead E L. Biomass burning: a driver for global change. *Environmental Science & Technology* 1995; 29: 120A-125A.

Luo W Q. Briefly on the atmospheric pollution and its control by burning coals. *Energy saving technology* 2008; 26: 267-268.

Li S S. Problems and countermeasures of the harmful trace elements in Chinese coal. *Coal science and technology* 2006; 34(1): 28-31.

Li X Y, Gilmour P S, Donaldson K, MacNee W. In vivo and in vitro proinflammatory effects of particulate air pollution (PM₁₀). *Environmental Health Perspectives* 1997; 105: 1279-1283.

Lin Z Q, Xi Z G, Chao F H. Research progress in the toxicity effects of the nano particles. *Journal of Preventive Medicine of Chinese People's Liberation Army* 2007; 25: 383-386.

Liu Y W, Mao X L, Sun L Y, Ni J R. Characteristics of heavy metals discharge from industrial pollution sources in Shenzhen. *Acta Scientiarum Naturalium Universitatis Pekinensis* 2010; 46: 279-285.

Loomis D, Grosse Y, Lauby-Secretan B, Ghissassi F E, Bouvard V, Benbrahim-Tallaa L, Guha N, Baan R, Mattock H, Straif K. The carcinogenicity of outdoor air pollution, *Lancet Oncology* 2013; 14:1262-1263.

Lu S L, Shao L Y, Wu M H, Jones, T P, Merolla L, Richard, R J. The related research of the bioactivity and trace elements of PM₁₀ in Beijing. *Science in China D: Geochemistry* 2006; 36(8): 777-784.

Merolla L, Richards R J. In vitro effects of water-soluble metals present in UK particulate matter. *Experimental Lung Research* 2005; 31: 671-683.

Moreno T, Merolla L, Gibbons W, Greenwell L, Jones T, Richards R. Variations in the source, metal content and bioreactivity of technogenic aerosols: a case study from Port Talbot, Wales, UK. *Science of Total*

Environment 2004; 333: 59–73.

Neas L M. Fine particulate matter and cardiovascular disease. *Fuel Processing Technology* 2000; 65-66: 55-67.

Ostro B, Broadwin R, Green S, Feng W Y, Lipsett M. Fine particulate air pollution and mortality in nine California counties: Result from CALFINE. *Environmental Health Perspectives* 2006; 114(1): 29-33.

Pui D Y H, Chen S C, Zuo Z. PM_{2.5} in China: Measurements, sources, visibility and health effects, and mitigation. *Particuology* 2014; 13: 1-26.

Querol X, Zhuang X, Alastuey A, Viana M, Lv W, Wang Y, Lopez A, Zhu Z, Wei H, Xu S. Speciation and sources of atmospheric aerosols in a highly industrialised emerging mega-city in Central China. *Journal of Environmental Monitoring* 2006; 8: 1049-1059.

Ren D Y, Zhao F H, Dai S F, et al. *The Trace Element Geochemistry of Coal*, Beijing: Science Press; 2006.

Reche C, Moreno T, Amato F, Viana M, van Drooge B L, Chuang H C, et al.. A multidisciplinary approach to characterise exposure risk and toxicological effects of PM₁₀ and PM_{2.5} samples in urban environments. *Ecotoxicology and Environmental Safety* 2012; 78: 327-335.

Samet J M, Dominici F, Curreiro F C, Coursac I, Zeger S L. Fine particulate air pollution and mortality in 20 US cities, 1987-1994. *The New England Journal of Medicine* 2000; 343: 1742-1749.

Sánchez-Pérez Y, Chirino Y I, Osornio-Vargas A R, Morales-Bárceñas R, Gutiérrez-Ruiz C, Vázquez-López I, et al.. DNA damage response of A549 cells treated with particulate matter (PM₁₀) of urban air pollutants. *Cancer Letters* 2009; 278(2): 192-200.

See S W, Wang Y H, Balasubramanian R. Contrasting reactive oxygen species and transition metal concentrations in combustion aerosols. *Environmental Research* 2007; 103: 317-324.

Shao L Y, Hu Y, Wang J, Hou C, Yang Y Y, Wu M Y. Particle-induced oxidative damage of indoor PM₁₀ from coal burning homes in the lung cancer area of Xuan Wei, China. *Atmospheric Environment* 2013; 77: 959-967.

Shao L Y, Jones T P, Gayer R A, Dai S F, Li S S, Jiang Y F. Petrology and geochemistry of the high-sulphur coals from the Upper Permian carbonate coal measures in the Heshan Coalfield, southern China. *International Journal of Coal Geology* 2003; 55: 1-26.

Shao L Y, Li J J, Zhao H Y, Yang S S, Li H, Li W J, Jones T P, Sexton K, Bérubé K A. Associations between particle physicochemical characteristics and oxidative capacity: an indoor PM₁₀ study in Beijing, China. *Atmospheric Environment* 2007; 41: 5316–5326.

Shao L Y, Shi Z B, Jones T P, Li J J, Whittaker A G, Bérubé K A. Bioreactivity of particulate matter in Beijing air: results from plasmid DNA assay. *Science of The Total Environment* 2006; 367: 261-272.

Straif K, Baan R, Grosse Y, Secretan B, El Ghissassi F, Coglianò V. Carcinogenicity of household solid fuel combustion and of high-temperature frying. *The Lancet Oncology* 2006; 7: 977-978.

Sun Z Q, Shao L Y, Mu Y J, Hu Y. Oxidative capacities of size-segregated haze particles in a residential area of Beijing. *Journal of Environmental Sciences* 2012; 26: 167–174.

Tang X Y, Huang W H. *Trace elements in coal in China*, Beijing: The commercial press; 2004.

Vidrio E, Phuah CH, Dillner A M, Anastasio C. Generation of hydroxyl radicals from ambient fine particles in a surrogate lung fluid solution. *Environmental Science & Technology* 2009; 43: 922-927.

Wang J, Shao L Y, Geng C M, Wang J Y, Liu J X, Yang W, Hu Y. Oxidative capacity of PM₁₀ emitted by burning coals. *Journal of Central South University (Science and Technology)* 2014; 45(6): 2137-2143 (in Chinese)

Whittaker A G. *Black smokes: Past and present*. The Thesis for the Degree of Ph.D. Cardiff University, 2003.

Xiao Z H, Shao L Y, Zhang N, Wang J, Wang J Y. Heavy metal compositions and bioreactivity of airborne

PM₁₀ in a valley-shaped city in northwestern China. *Aerosol and Air Quality Research* 2013; 13: 1116–1125.

Xu M H, Yan R, Zheng C G, Qiao Y, Han J, Sheng C D. Status of trace element emission in a coal combustion process: a review. *Fuel Processing Technology* 2003; 85: 215-237.

Zhang W L, Xu D Q, Cui J S. Air pollutant PM_{2.5} monitoring and study on its genotoxicity. *Journal of Environment and Health* 2003; 1: 3–4.

Zhong C Y, Zhou Y M, Smith K R, Kennedy I M, Chen C Y, Aust A E, Pinkerton K E. Oxidative injury in the lungs of neonatal rats following short-term exposure to ultrafine iron and soot particles. *Journal of Toxicology and Environmental Health, Part A: Current Issues* 2010; 73: 837-847.

Tables:

Table 1. Information of the proximate and ultimate analysis of the raw coals used in this study

Table 2. Mass concentration of the PM₁₀ emitted by burning different coals (μg/m³)

Table 3. Percentage of DNA damage induced by the PM₁₀ emitted from burning different fuels

Table 4. Contents of water-soluble trace elements in the intact whole PM₁₀ emitted from burning different types of coal and wood charcoal (ppm)

Table 5. Correlation coefficients between the total and individual water-soluble heavy metal concentrations and the percentages of DNA damage by coal-burning PM₁₀

Table 6. Toxic index of the PM₁₀ emitted by burning different coals

Figures:

Fig.1 Sketch diagram showing composition of the coal combustion stove system which contains a stove, a dilution tunnel and the smoke chambers. “HC” represents honeycomb briquette; “RC” represents raw powdered coal.

Fig.2 A comparison between the morphology and the quantity of PM₁₀ emitted by burning honeycomb briquette and raw powdered coal. DT-H and ZJ-H represent Datong and Zhijin honeycomb briquettes respectively, DT-R and ZJ-R represent Datong and Zhijin raw powdered coals respectively.

Fig.3 Gel images and histograms of the oxidative damage on DNA that was induced by PM₁₀ emitted by burning different fuels. (“a” represents ZJ honeycomb briquette; “b” represents DT honeycomb briquette; “c” represents ZJ powder coal; “d” represents DT powder coal; “e” represents DS powder coal; “f” represents YC powder coal; “g” represents JX powder coal; “h” represents wood charcoal; “W” represents the whole-particle suspension; and “S” represents the water soluble fraction).

Fig. 4. Comparison between the DNA damage percentages of the whole particles and the water-soluble fraction of the coal burning-derived PM₁₀ under a dose of 500mgml⁻¹ (“H” represents honeycomb briquette, “R” represents raw powdered coal).

570

Table 1. Information of the proximate and ultimate analysis of the raw coals used in this study

	Proximate analysis						Ultimate analysis				
	moisture %	ash content %	Volatiles %	Fixed carbon %	Higher heating value MJ/kg	Lower heating value MJ/kg	S%	C%	H%	N%	O%
Coal of ZJ	0.94	9.08	5.76	84.22	31.82	31.23	2.24	81.86	2.76	1.04	2.08
Coal of DT	6.98	9.50	32.07	51.45	27.12	26.19	0.21	64.6	3.56	0.84	14.31
Coal of DS	7.46	6.68	30.82	55.04	28.45	27.51	0.20	68.72	3.76	0.90	12.28
Coal of YC	1.30	23.28	19.74	55.68	19.85	19.51	0.36	62.68	2.16	0.62	9.60
Coal of JX	3.02	26.34	4.44	66.20	22.96	22.73	0.25	68.26	0.79	0.26	1.08

571 Note: the above content is for the air dry basis of coal; “ZJ” represents Zhijin; “DT” represents Datong; “DS” represents

572 Dongsheng; “YC” represents Yinchuan; and “JX” represents Jingxi.

573

574

Table 2 Mass concentration of the PM₁₀ emitted by burning different coals (μg /m³)

Fuel types	Mass (μg)	flow rate (L/min)	sampling time (min.)	mass concentration (μg/m ³)
ZJ-H	7800	78	78	1282.05
DT-H	4300	78	80	689.10
ZJ-R	13400	78	60	2863.25
DT-R	18100	78	56	4143.77
DS-R	34200	78	41	10694.18
YC-R	16100	78	29	7117.60
JX-R	5600	78	50	1435.90

575

Note: H represents honeycomb briquettes; R represents raw powdered coal.

576

577
578

Table 3. Percentages of DNA damage induced by the PM₁₀ emitted from burning different fuels

Fuel Types	Samples status	Dosage of PM ₁₀ (μg/ml)				
		25	50	100	300	500
ZJ-H	Whole-particle suspension (%)	12.46(±0.69	30.70(±1.67	33.03(±1.48	38.61(±2.49	55.37(±1.91
)))))
	Water-soluble fraction (%)	14.05(±0.02	23.42(±1.05	25.89(±0.75	36.73(±0.89	48.34(±1.40
)))))
DT-H	Whole-particle suspension (%)	12.29(±1.14	11.95(±1.75	26.22(±0.22	37.85(±1.18	46.08(±1.34
)))))
	Water-soluble fraction (%)	10.98(±0.94	11.35(±2.09	22.54(±0.38	34.10(±1.58	44.97(±1.70
)))))
ZJ-R	Whole-particle suspension (%)	13.32(±0.36	15.18(±0.39	17.17(±1.11	23.18(±1.43	33.73(±1.22
)))))
	Water-soluble fraction (%)	8.58(±0.37)	9.63(±0.71)	11.79(±1.39	23.81(±0.30	23.61(±0.98
)))))
DT-R	Whole-particle suspension (%)	12.55(±0.24	13.59(±0.18	13.44(±0.60	20.09(±0.64	19.37(±0.15
)))))
	Water-soluble fraction (%)	7.70(±0.46)	9.86(±0.04)	9.30(±0.16)	12.37(±0.37	15.60(±0.92
)))))
DS-R	Whole-particle suspension (%)	10.33(±0.65	11.29(±0.25	12.24(±0.06	14.27(±0.18	16.85(±0.45
)))))
	Water-soluble fraction (%)	7.58(±0.06)	10.14(±0.86	12.46(±0.91	13.57(±0.04	15.52(±0.13
)))))
YC-R	Whole-particle suspension (%)	15.68(±1.85	16.62(±0.27	20.70(±0.45	31.89(±0.74	33.70(±1.14
)))))
	Water-soluble fraction (%)	20.66(±1.26	22.51(±0.79	23.02(±0.28	25.52(±0.43	30.01(±1.49
)))))
JX-R	Whole-particle suspension (%)	6.83(±0.81)	8.84(±0.79)	11.65(±0.67	14.71(±0.83	16.37(±0.50
)))))
	Water-soluble fraction (%)	4.84(±0.74)	7.45(±0.26)	8.85(±1.38)	10.72(±0.83	12.21(±1.11
)))))
wood charcoal	Whole-particle suspension (%)	11.37(±0.93	12.25(±0.07	14.48(±0.69	15.55(±0.13	16.99(±1.05
)))))
	Water-soluble fraction (%)	11.61(±1.01	11.89(±0.75	13.15(±0.20	13.95(±1.42	14.38(±0.25
)))))

579
580

Note: “H” represents honeycomb briquettes, “R” represents raw powdered coal, “±” represent error range

581

Table 4. Contents of water-soluble trace elements in the intact whole PM₁₀ emitted from burning different types of coal and

582

wood charcoal (ppm)

	ZJ-H	DT-H	ZJ-R	DT-R	DS-R	YC-R	JX-R	Wood charcoal
As	412	155	19.6	19.9	18.3	46.5	9.46	19.7
Cd	93.6	15.8	10.3	0.08	0.23	19.8	0.6	0.3
Cr	1.92	9.08	9.36	8.02	3.09	5.2	3.99	13.5
Co	0.6	1.92	0.15	0.63	1	0.23	0.02	—
Cs	2.57	6.42	2.97	4.48	2.3	5.9	3.88	5.34
Cu	86.4	16.2	278	12.4	8.69	18.8	15.3	16.5
Ge	890	37.5	7.88	2.86	2.71	1.08	0.471	0.74
Mn	16.6	30.5	12.2	0.42	1.44	8.76	3.79	—
Mo	13	5.02	3.73	7.36	7.57	7.5	2.56	2
Ni	47.4	22.7	22.9	13.6	19	8.37	18.8	13.1
Pb	2385	824	324	0.39	2.12	77.1	3.39	16
Se	61.3	43.2	10.5	12	2.57	4.16	1.5	8.88
Sr	8.28	7.86	12.3	3.15	2.23	10.1	5.42	14
Sb	46.5	14.8	0.93	1.92	9.38	4.21	1.16	0.75
Ti	84.1	19.5	61.5	29.2	65.2	20.5	56.6	3.16
Tl	179	98.1	9.86	2.76	1.73	16.5	2.19	4.83
V	2.36	1.13	1.87	1.9	1.59	4	1.39	2.5
Zn	17150	4350	2408	98.2	63.5	3702	71	18.8
Total	21480.63	5658.73	3196.05	219.28	212.65	3960.71	201.52	140.11

583

Note: “—”represents that the measured values of the corresponding element are below the detection limit. “Total” represents

584

sum of the analysed elements. “H” represents honeycomb briquettes. “R” represents raw powdered coal.

585

Table 5. Correlation coefficients between the total and individual water-soluble heavy metal concentrations and the percentages of DNA damage by coal-burning PM₁₀

588

589

Table 6. Toxic index of the PM₁₀ emitted by burning different coals

Fuel types	mass concentration ($\mu\text{g}/\text{m}^3$)	percentage of DNA damage at 500 $\mu\text{g}/\text{ml}$ dose	toxicity index
ZJ-H	1282.05	55.37	70987
DT-H	689.10	46.08	31754
ZJ-R	2863.25	33.73	96577
DT-R	4143.77	19.37	80265
DS-R	10694.18	16.85	180197
YC-R	7117.60	33.70	239863
JX-R	1435.90	16.37	23506

590

Note: “H” represents honeycomb briquette, “R” represents raw powdered coal.

591

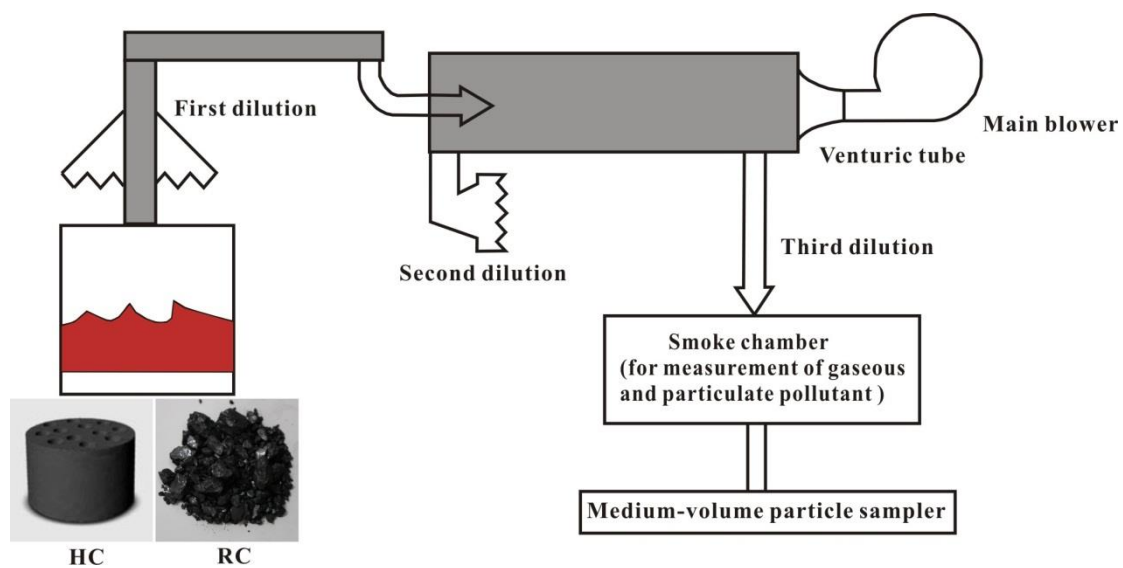


Fig.1 Sketch diagram showing composition of the coal combustion stove systems which contains a stove, a dilution tunnel and the smoke chambers. "HC" represents honeycomb briquette; "RC" represents raw powdered coal

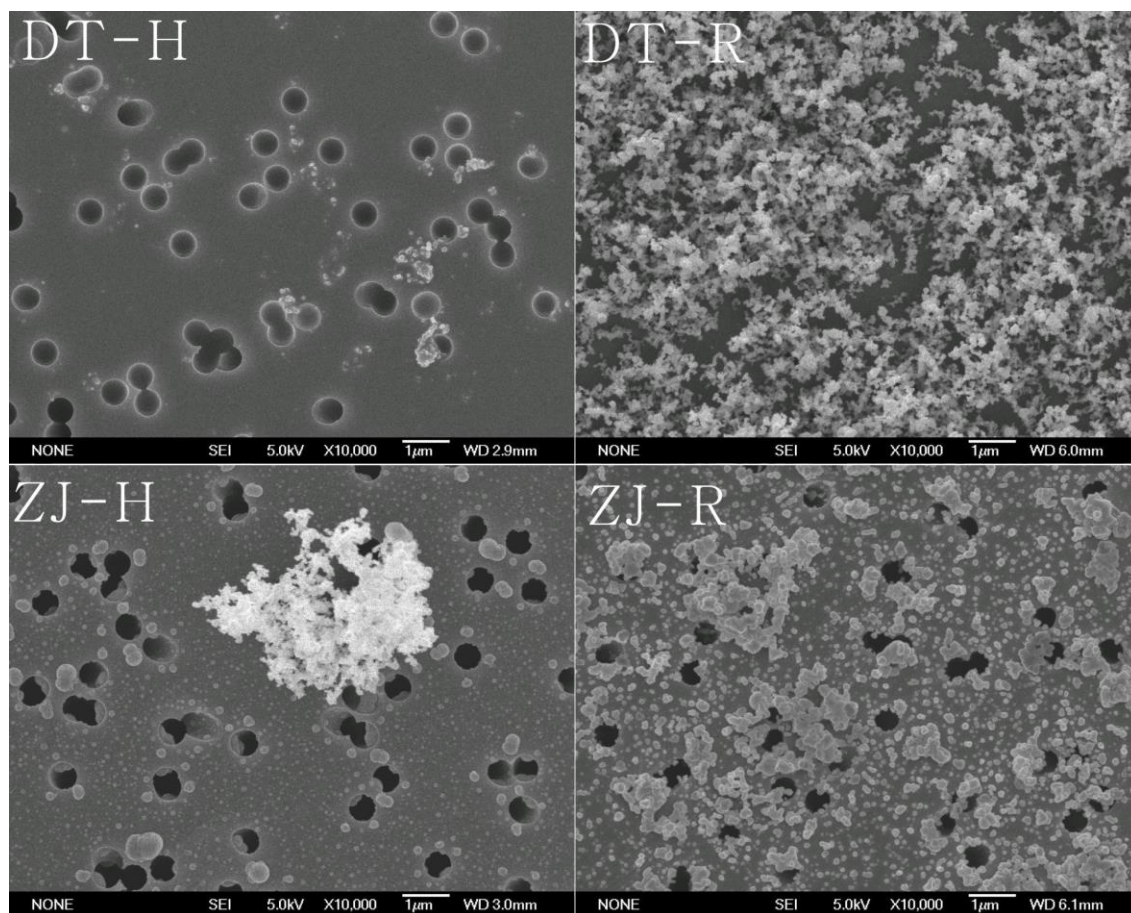


Fig.2 A comparison between the morphology and the quantity of PM₁₀ emitted by burning honeycomb briquette and raw powdered coal. DT-H and ZJ-H represent Datong and Zhijin honeycomb briquettes respectively, DT-R and ZJ-R represent Datong and Zhijin raw powdered coals respectively.

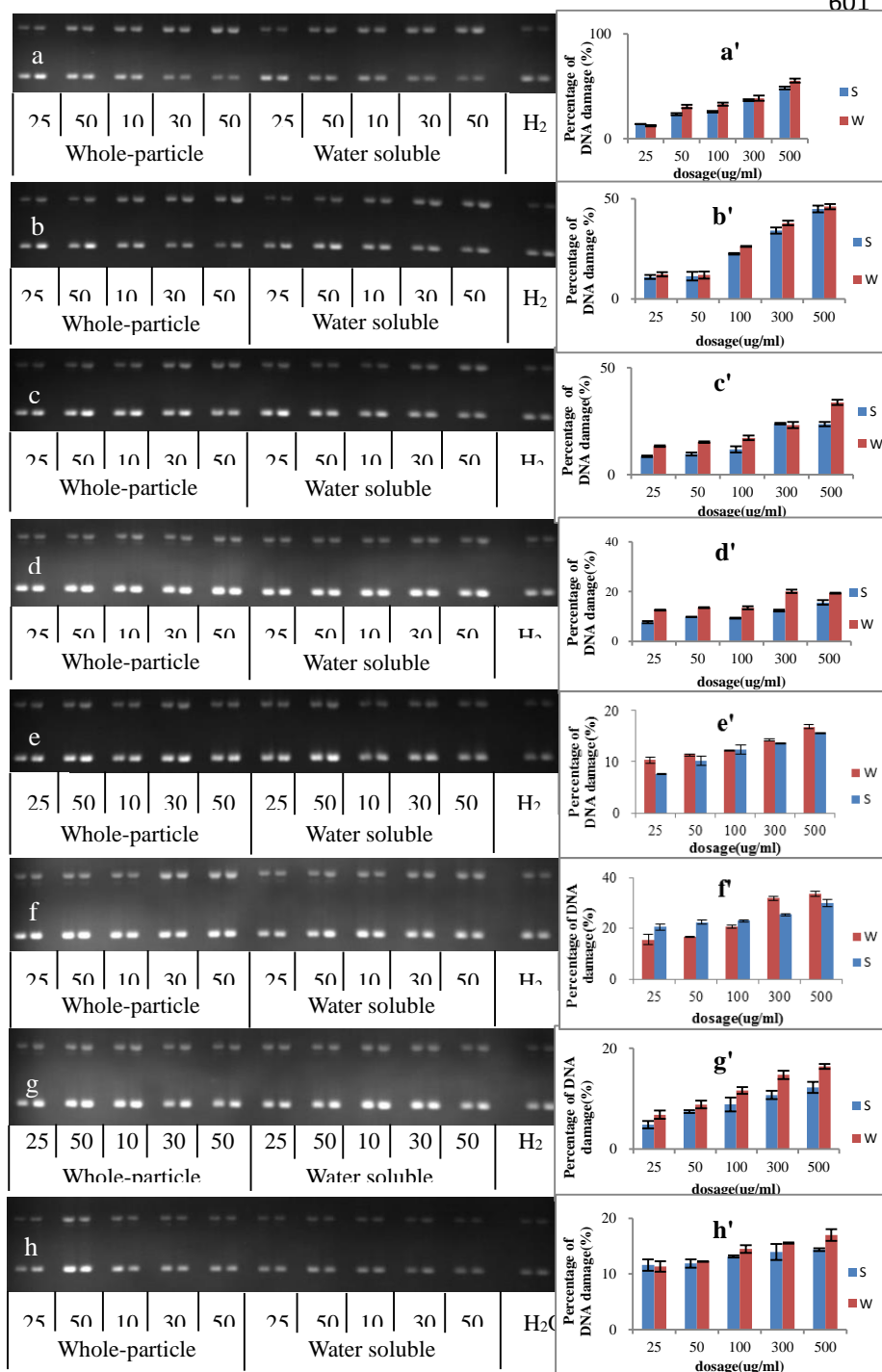


Fig.3 Gel images and histograms of the oxidative damage on DNA that was induced by PM₁₀ emitted by burning different fuels. (“a” represents ZJ honeycomb briquette; “b” represents DT honeycomb briquette; “c” represents ZJ powder coal; “d” represents DT powder coal; “e” represents DS powder coal; “f” represents YC powder coal; “g” represents JX powder coal; “h” represents wood charcoal; “W” represents the whole-particle suspension; and “S” represents the water soluble fraction).

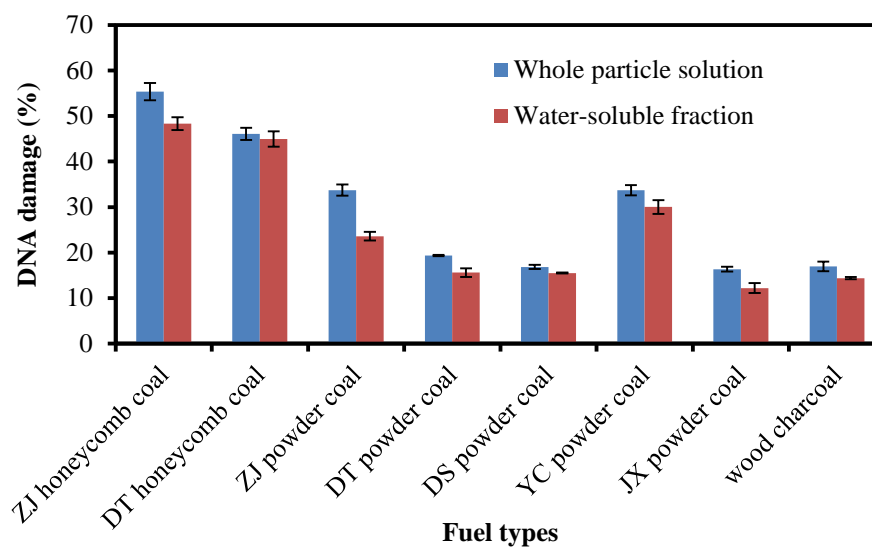


Fig. 4. Comparison between the DNA damage percentages of the whole particles and the water-soluble fraction of the coal burning-derived PM₁₀ under a dose of 500mgml⁻¹.